Chapter 3: Methods and Models of Quantum Dot Synthesis

Summary

Since QD emission is size dependent, colloidal growth must be carefully controlled to achieve the target average radius with a narrow particle size distribution. A variety of methods have been developed to make semiconductor nanocrystals, including arrested precipitation in water. Then organometallic synthesis routes were pioneered[24] and modified[33] to produce superior crystallinity and higher photoluminescence quantum yield (PLQY)[14,34] from higher temperature reactions, and to provide better size control and surface passivation,[34,35] all by growing QDs in trioctylphosphine oxide (TOPO) rather than in water. Many studies have been performed to optimize quantum dot performance by varying synthesis parameters (such as reaction solvent composition, precursor concentration, and temperature) that affect reaction kinetics.[36]

Using thermodynamics, the Gibbs-Thompson equation helped explain why size distributions could widen with synthesis time, if reactant concentrations were depleted below the QDs' size-dependent solubility threshold.[29,37,38] Early theoretical studies of nanocrystal growth rates emphasized Ostwald ripening,[39,40,41,42] whereby larger particles grow and smaller particles dissolve, thus widening particle size distributions when reactants are scarce. Researchers concluded that narrower size distributions could be achieved when nanocrystal growth was limited by diffusion rather than by reaction rate.[29,43] The rate at which material is transported by diffusion and is incorporated by a surface reaction can be expressed in very similar forms, which must be equated to satisfy

conservation of matter. From this, Weller's group developed a comprehensive model using several activation energies to simulate QD size evolution under a wide variety of organometallic synthesis conditions.[43]

Survey of Synthesis Methods

Even before the recent popularization of quantum dots, a theoretical framework for the growth of nanoparticles was developed with many helpful insights as to the conditions needed for narrow size distributions. For example, coagulation should be minimized, nucleation and growth should occur separately, and diffusion control would be preferred over reaction control for narrow particle size distributions.[37]

Coagulation occurs when small bare particles touch and fuse in order to reduce their surface area. In general, coagulation can be prevented by adding appropriate coatings around each of the particles to improve their suspension in the solvents and cause them to repel each other by columbic forces or steric hindrance.[37]

Ideally, nucleation should stop before significant growth begins. If small nuclei continue to form as larger particles grow, then the size distribution would widen with time.[37]

Methods for preparing colloidal CdSe quantum dots can be divided into two categories depending on the nature of the solvent. Wet chemistry uses low-temperature polar solvents such as water or methanol. Organometallic synthesis uses high temperature, non-polar solvents such as trioctylphosphine oxide (TOPO). Within each category, there are numerous variations in the exact precursors, solvents, and special additives, as well as in the temperatures and pressures required. Although all of the

methods discussed below can be scaled up for commercial production,[44] the wet chemistry routes generally produce lower quality nanocrystals, with smaller and wider photoluminescence emission peaks.

In wet chemistry routes, the synthesis temperature is limited by the boiling point of the solvent. Growing at lower temperatures produces quantum dots with higher defect concentrations, which translates into a low PLQY. The particle size distributions are usually so wide that size-selective precipitation is required to separate a distribution into sections with narrow emission peaks.[44]

Perhaps the most popular and successful aqueous method is arrested precipitation, which has been used to synthesize a wide range of semiconductor nanocrystals, including CdS,[45] CdSe,[46] CdTe, and HgTe.[4,7] Cadmium perchlorate is dissolved in water and hydrogen selenide gas. Through this solution, HSe gas is bubbled for many hours. Then, the double replacement reaction yields CdSe nanocrystals in solution. NaOH is added to make the solution alkaline. Additives such as phosphates, amines, and thiols protect the quantum dots, enhance their suspension in water, stabilize the reaction, and control growth, resulting in reasonably bright and narrow PL emission.[44]

Alternatively, Se metal can be reduced to an ion by KBH_4 and combined with a cadmium salt in ethylenediamine at room temperature to produce amine-capped nanocrystals from 4 nm to 6 nm in diameter and with low crystallinity.[44]

Ultrasound cavitation and electrochemical stimulation enhance the formation of CdSe nanocrystals from selenourea and cadmium acetate precursors in water.[44]

Solvothermal processes use pressure vessels to elevate the maximum synthesis temperature for better crystallinity. Cd precursors such as cadmium carbonate, cadmium

nitrate, and cadmium sulfate can be dissolved in water, ethanol, tetrahydrofuran, butane-1,4-diol, or ethylene glycol. For spherical particles rather than rods, solvothermo temperatures must stay below 120 ^{o}C in these solvents.[44]

In a nonpolar variation of the solvothermal process, dodecanethiol capping ligand, cadmium stearate, and selenium metal are combined and heated under pressure in tetralin. The tetralin converts to naphthalene, producing a necessary hydrogen selenide precursor. The resulting CdSe quantum dots suspend well in toluene and other nonpolar solvents, and the nanocrystals are about 3 nm in diameter, but the size distributions are still rather wide after solvothermo formation.[44]

More popular organometallic routes were developed to form CdSe quantum dots and then extended to CdTe,[24,33,34,46] but not to HgTe. Authors have adapted the original organometallic method developed by Bawendi's group.[4] Unfortunately, the first Cd precursor was dimethyl cadmium, which is very dangerous. "$Cd(CH_3)_2$ is extremely toxic, pyrophoric, expensive, unstable at room temperature, and explosive at elevated temperatures by releasing large amount of gas," according to Peng and Peng, who introduced CdO as a safer replacement.[33] CdO is dissolved in TOPO above 300 ^{o}C, while Se metal dissolves in TOPO at room temperature. Once the Se solution is injected into the hot Cd solution, the reaction typically proceeds at temperatures below 300 ^{o}C.

Variations on organometallic synthesis have been developed using different Cd precursors. A wide variety of weak cadmium salts (such as cadmium oxide, cadmium acetate, and cadmium carbonate) can be dissolved in alternative high temperature solvents (such as a phosphonic acids, fatty acids, or amines) at temperatures from 220 to 340 ^{o}C.[47] Despite their solubility in the reaction solvents, other cadmium sources, such

as chlorides, sulfates, or thiolates, produce only coarse CdSe precipitates but no nanocrystals.[47] If the cadmium complex interaction bond is too strong, then quantum dot growth is not feasible.[47] The Cd-ligand complex must be less stable than CdSe in order for the synthesis reaction to have a driving force to proceed.

Comparing Oganometallic Synthesis vs. Arrested Precipitation

In the vast majority of all published research on CdSe quantum dots, either oganometallic synthesis or arrested precipitation is used. The success of these two methods originates from the behavior of the ligands. Ligands keep the particles isolated, thus preventing nuclei agglomeration and facilitating homogeneous growth. Nanocrystal size variations are reduced when ligands control the growth rate of particles. Ligands passivate the surface. Organic ligands that bind to the surface during organometallic synthesis naturally provide surface passivation, which protects the surface from oxidation and minimizes the electronic trapping properties of surface defects, both of which help to maintain high PLQY. Aqueous synthesis can also be designed to surround QDs with hydrophilic ligands that may protect against oxidation after the water has evaporated.[44]

A more detailed review of the advantages and disadvantages of these two approaches may suggest which route is preferred for making nanocrystals for biomedical or photonic applications.

Several factors favor arrested precipitation, including fewer environmental and safety hazards, and the economical scalability of the process to commercial production levels. Also, quantum dots formed in water are suspended in water from the start, which is desirable for labeling proteins in a biological system. However, the reaction

temperature in water may not exceed 100 ^{o}C (at atmospheric pressure). This limits the mobility of add-atoms on the surface of growing nanocrystals, resulting in defects in the crystal structure. Defects may act as nonradiative recombination sites for electron-hole pairs produced by incident excitation light, thereby reducing the PLQY of the quantum dots. To improve the PLQY, nanocrystals formed by arrested precipitation may be given a post-processing heat treatment.[4,48]

After formation in water, the PLQY of nanocrystals can decrease significantly with exposure to oxygen or organic solvents.[48] Lower PLQY translates directly into poor performance in photonic and biomedical applications. Decreases in PLQY may be caused by degradation of exposed surfaces through the formation of metal oxides.[49] In biomedical applications, soluble heavy-metal oxides kill cells.[13] The migration of surface material in aqueous solutions may also alter the particle size and emission wavelength distribution.[4] So, for biological safety, chemical stability, and higher efficiency, the quantum dot surface should be passivated by a layer that will satisfy dangling bonds and will transmit light in and out of the nanocrystal. In addition to the organic passivation from ligands, an inorganic shell of ZnS can be grown around the CdSe core[50] as an extra step in either method. Surrounding the CdSe core with a wide-bandgap semiconductor shell provides long-term chemical stability, high PLQY, and shorter radiating emission lifetimes.[44]

Depending on the application, quantum dots may need to be suspended in a particular solvent. Biomedical applications usually involve aqueous environments. Photonic applications for quantum dots rarely require suspension in water, and organic solvents are often needed during the fabrication of devices with polymer-nanocrystal

composite layers. Of course, quantum dots made by wet chemistry routes are readily resuspended in water and other polar solvents. Generally, quantum dots formed via organometallic synthesis can be resuspended in a variety of volatile non-polar organic solvents, because of the residual non-polar organic ligands bonded to the nanocrystal surface.

Oleic acid and eladic acid have provided significantly better protection against oxidation and emission loss than octadecylamine (ODA) or stearic acid, although all four have the same chain length, with 18 carbons. The high stability of quantum dots coated with oleic acid was attributed to an amorphous structure of the ligand layer. Likewise, branched ligands also provided high chemical stability.[51] Fourier Transform Infrared (FTIR) spectra indicated that stearic acid ligands around a quantum dot packed in a way similar to crystallized paraffin. Researchers suggested that an amorphous ligand layer was less permeable to oxygen than a crystalline ligand layer.[51]

For biomedical applications, one of the challenges being addressed is modifying quantum dots made via organometallic synthesis so they will suspend in aqueous biological environments. Various ligand replacement schemes have been developed to transfer "solubility" (the quantum dots are actually *suspended*, not dissolved) from non-polar to polar solvents.[52] However, during this transfer quantum dots are vulnerable to oxidation, which degrades their PLQY dramatically, especially for CdSe without a ZnS shell. Even with a protective ZnS shell, CdSe quantum dots exhibit a reduction in PLQY, from 50% to 20±10%, when TOPO ligands are replaced by hydrophilic ligands.[53] CdSe is more vulnerable during ligand replacement than CdTe.[51] A more robust solution is to surround the entire core-shell-ligand structure in a phospholipid micelle, which is

hydrophobic on the inside and hydrophilic on the outside, like a detergent. CdSe-ZnS core-shell quantum dots show a PLQY of 24% after suspension in water by micelles.[54]

Organometallic synthesis has several advantages over arrested precipitation. In organometallic synthesis, nucleation does not continue during the growth stage, which helps the size distribution remain narrow. At the higher temperatures allowed by organometallic synthesis, reaction rates are faster and crystallinity is generally higher. In industry, time is money, so some of the economies of scale that favor arrested precipitation are offset by long reaction times, measured in days or weeks in water, compared to minutes in TOPO. At higher temperatures, there is more thermal energy to help each add-atom find more energetically favorable bonding positions in the crystal lattice, thus reducing defects by annealing during growth. This often translates into higher PLQY. CdTe quantum dots made via organometallic synthesis have PLQYs from 50% to 65%, which is significantly higher than 18% [34] or 3% – 10% [53] via arrested precipitation. The PLQY of CdSe quantum dots without ZnS shells has been extended up to 85% via organometallic synthesis,[1] which surpasses the low PLQY of CdSe nanocrystals without ZnS shells made via arrested precipitation.[53] Even with ZnS shells, CdSe quantum dots made via arrested precipitation have only reached a PLQY of 70%.[50] Presumably, adding a ZnS shell during optimized organometallic synthesis of CdSe should increase the PLQY above 85%. The need for high performance in photonic and biomedical applications favors organometallic synthesis for CdSe quantum dots.

Effects of Varying Organometallic Synthesis Parameters

In order to produce CdSe quantum dots with carefully controlled shape, crystal structure, size, and crystallinity, it is important to understand how nucleation and growth are affected by experimental conditions. Although the focus here is on CdSe quantum dot growth, some examples from the similar CdTe materials system are used when necessary to illustrate general principles.

For most applications that were discussed in Chapter 1, nanospheres are more desirable than nanorods, because nanospheres can achieve a higher PLQY (85% for CdSe without ZnS shell[1]) than nanorods (1% for CdSe without ZnS shell[55] or ~20% for CdSe with ZnS shell[51]). Sharp nanorods might cause more physical damage to cells and might accumulate more in cells than nanospheres.[56] The Cd precursor concentration and solvent affect nanocrystal shape. Spherical nanocrystals are produced as long as the concentrations of precursors and strongly binding coordinating ligands (such as tetradecyl-phosphonic acids (TDPA) and hexyl-phosphonic acids (HPA)) are below some threshold; higher concentrations are necessary but not sufficient to yield asymmetric rods or tetrapods in both the CdSe and CdTe systems.[36,38,51,57]

In the CdTe system, nanoparticle shape has been investigated in alternative solvents for Cd and Te precursors. When CdO is dissolved in oleic acid, the shape is sensitive to the phosphine chain length in the solvent used to dissolve Te, even though no phosphine groups are attached to the final nanoparticles. When CdO is dissolved in phosphonic acids such as octadecylphosphonic acid (ODPA) and TDPA, nanocrystals are always spherical regardless of Cd concentration or phosphine chain length. However, dissolving CdO in a traditional mixture of TOPO and TDPA can enable rod formation.

Dissolving Te in tributylphosphine or trihexylphosphine consistently produces spheres; but high concentrations of Te in trioctylphosphine (TOP) can yield rods,[51] so longer chained solvents can lead to asymmetric growth. Development of a clear theoretical understanding of quantum dot shape evolution is still an area of active research, but Peng & Peng assert that traditional facet surface energy concepts are irrelevant for determining the shape of CdSe nanocrystals during organometallic synthesis, because this is a nonequilibrium process.[38]

Quantum dot crystal structure can be controlled by the choice of the main reaction solvent and temperature. For example, CdSe nanocrystals grown in TOPO or fatty acids generally have the wurtzite structure, while zincblende structures are often observed in CdSe quantum dots grown in amines at the same low temperatures (170–220 ^{o}C).[47] When amines with progressively higher molecular weight are used as the reaction solvent, progressively higher temperatures are needed to produce wurtzite CdSe quantum dots.[1] In CdTe nanocrystals, using oleic acid as the Cd ligand produces wurtzite at higher temperatures, but using ODPA produces a zincblende structure at lower temperatures.[51] Luckily, crystal structure does not seem to affect the PLQY of CdTe quantum dots.[51] To interpret these observations, the following explanation has been proposed. For both CdSe and CdTe, zincblende seems to be energetically preferred, so conditions which produce slow growth rates tend to yield this more stable crystal structure. However, as nanocrystals grow larger than a critical radius, a transformation to wurtzite (with zincblende stacking faults) is possible.[51] This transformation is more probable under conditions that lead to high growth rates.

CdSe and CdTe nanocrystal growth rate is affected by the choice of the solvent for Cd and the solvent for Se or Te. Peng and Peng observed that the "type and concentration of the strong Cd ligands added play a very important role in determining the growth rate."[58] Why does the Cd ligand play such a leading role? FTIR spectra show that quantum dots are coated by the ligand used to dissolve the CdO, not the ligand used to dissolve the Te (or Se).[51] In the absence or in very low concentrations of strong ligands such as TDPA, the growth rate is progressively faster in progressively shorter-chained fatty acids.[47] Whereas the growth rate is *directly* affected by the reaction solvent and the Cd precursor, there can be *indirect* effects from the Se or Te precursor via alterations in the nucleation rate.

Nucleation rate can be suppressed in following ways: decreasing the concentration of Se^{-2} or Te^{-2} ions, using a higher concentration of the Cd ligand, using a ligand with a physically longer chain, or using a stronger chemical "bond" between Cd and a ligand.[51] Higher nuclei concentrations occur when the initial Se concentration is higher.[38]

The coordinating solvent mixture strongly affects nucleation, which in turn affects QD growth. Bullen chose octadecene as a non-coordinating reaction solvent, so the effects of oleic acid ligands could be studied. CdO was dissolved in oleic acid (to form a cadmium oleate complex), while Se was dissolved in TOP or tributylphosphine. As the total oleic acid concentration was increased, the nuclei concentration decreased linearly, the average nuclei size increased, as did the growth rate. Higher concentrations of oleic acid may inhibit nucleation by capping nuclei more effectively and making it harder for

them to grow. After a small initial increase and decrease, the nuclei concentration remained fairly constant during the growth phase.[59]

When oleic acid is used to dissolve CdO, then dissolving Te (or Se) in a shorter chain length solvent, such as tributylphosphine or instead of trioctylphosphine, increases the nuclei concentration by a factor of ten. More nuclei consume Cd precursors faster during nucleation and during the initial stages of quantum dot growth, leaving less Cd available during later stages of growth. However when CdO is dissolved in a phosphonic acid, such as ODPA, the consumption of Cd proceeds slightly slower than in oleic acid, and the consumption rate during growth is independent of the Te (or Se) solvent chain length.[51] The slower nucleation and growth rate observed when CdO is dissolved in a phosphonic acid (rather than a fatty acid), is consistent with a stronger interaction strength between Cd and its two phosphonic acid ligands. When nucleation and growth rates are slowed by the strong phosphonic acid "bond," then increasing other rates, such as the diffusion of Te (or Se) in the reaction liquid, does not affect the net nucleation or growth rate. In this particular case, breaking strong Cd-ligand "bonds" is the rate-limiting step for quantum dot nucleation and growth.[51] As another example, "thiols, which are very strong ligands to cadmium, were found to inhibit the nucleation process."[51]

An automobile assembly line provides a good analogy of quantum dot growth. A production bottleneck behaves like a rate-limiting step. Efforts to ease bottlenecks (such as Cd-ligand interaction on the QD surface) can improve net productivity dramatically. On the other hand, increasing the circulation of nuts and bolts (such as using smaller

molecules to transport Se^{+2} ions) will not get more cars out the door if critical parts do not arrive on time.

To increase the rate-limiting step of surface interaction, smaller stabilizers, such as hexylphosphonic acid (HPA), are used rather than larger stabilizers, such as tetradecylphosphonic acid (TDPA); the result is faster CdSe nanocrystal growth in TOPO as the reaction solvent.[36] When CdSe nanocrystals are grown in a mixture of TOPO and TDPA (mostly TOPO), the nanocrystal surfaces become coated primarily with TDPA (the stronger ligand).[38] If CdO is dissolved in this same mixture, and the mixture is aged at room temperature for several days, then Cd-TDPA complexes gradually replace the more weakly bonded Cd-TOPO complexes. If this aged mixture is used in a reaction, CdSe quantum dots grow more slowly, because their surfaces contain higher levels of TDPA instead of TOPO.[38] In general, phosphonic acids yield slower reaction rates than TOPO or fatty acids, because the Cd-chelate complex from phosphonic acids has a stronger interaction energy than that of TOPO or fatty acids.[51]

During the growth phase, the emission peaks initially narrow with reaction time as the radius increases; however, after the particle size levels off, the PL emission full width at half maximum (FWHM) and the radius begins to increase later in the reaction.[59] There is a general consensus that the widening of PL emission peaks and the slight increase in growth rate later in a reaction indicate the onset of Ostwald ripening, as discussed later.[59]

Experimentally, the Cd:Se molar ratio and the total precursor concentration can be optimized to minimize particle size variation at a particular stage in quantum dot

growth.[29] This stage of narrowest width in the particle size distribution occurs when the reaction runs out of Cd precursor.[29]

PLQY is affected by several factors, including growth temperature, reaction solvent, Cd ligand, and the Cd:Se precursor ratio. Using standard methods (*i.e.* in TOPO with Cd:Se ~ 1:1.3), the PLQY of CdSe quantum dots with no ZnS shell only reaches a maximum of about 20% when the emission wavelength is between 520 and 600 nm, but the PLQY is generally very low for orange or red emitting nanocrystals.[1] Changing the reaction solvent to stearic acid moderately improves the best PLQY to 30%, but the PLQY still decreases for larger nanocrystals.[47] Of course, the PLQY can be increased to about 50% by passivating the surface with a ZnS shell.[1] This presents a problem in biomedical applications, where bright emitters at longer wavelengths are valued for their higher transmission through biological fluids.

Facing this challenge, Qu and Peng[1] set out on a quest for the brightest red-emitting CdSe quantum dots. Based on past experience, CdO was dissolved in stearic acid for high temperature synthesis, Se was dissolved in tributylphosphine, and various reaction solvent mixtures were explored. The reaction solvent contained TOPO (for low viscosity and easy processing), dioctylamine (for low toxicity), and a particular amine. Amines were generally more helpful than other solvents for producing bright CdSe quantum dots. Within the amine family, hexyldecylamine yielded the highest performance (PLQY ~ 85%), followed by octadecylamine (PLQY ~ 50–60%), and finally dodecylamine (with lower PLQY). The lower PLQYs correlated with the lower maximum allowed growth temperature without decomposition for each amine. To

improve post-synthesis stability of highly reactive amine ligands, "flexible dendron ligands with an amine group at their focal point are worth testing."[1]

Using the optimized solvent mixture with hexyldecylamine, Qu and Peng then varied the initial Cd:Se ratio. Increasing the Se concentration dramatically broadened the range of bright wavelengths and increased the maximum PLQY at the target wavelength of 620 nm. The following trends in the initial Cd:Se ratio (and PLQY) were observed: 1:10 (85%), 1:5 (75%), 1:1 (38%), and 2:1 (52%). The improvement in PLQY when the Cd:Se ratio was 2:1 was only over a very narrow wavelength range, so this is not the direction to go. In this study, the conditions for higher PLQY also produced narrower emission peaks.[1]

As reaction time progressed, the FWHM of photoluminescence emission gradually decreased and the PLQY gradually increased to their optimum levels. Longer reaction times produced progressively lower PLQY and higher FWHM, as Ostwald ripening began. Often the minimum FWHM occurred earlier than the maximum PLQY, but the FWHM usually remained low and did not significantly increase until the PLQY reached its maximum.[1] Understanding trends in PLQY and FWHM for CdSe quantum dots is important to optimize performance in applications and to evaluate growth mechanisms. Therefore, trends in PLQY and emission width will be analyzed as a function of temperature in Chapters 6 and 7.

Reductions in PLQY are expected to be associated with defects. It is important to note that PLQY is not affected by one kind of crystal defect, namely by zincblende stacking faults in wurtzite CdSe nanocrystals.[1] Surface states are therefore emphasized as a potential source of traps for carriers, resulting in nonradiative recombination.

Certain ligands may decrease the interaction of carriers with these traps for brighter emission. Passivation of the surface can explain the general increase in the PLQY, but it does not explain the sequential increase and decrease of PLQY as a function of synthesis time. Perhaps the physical packing of ligands affects the atomic structure of quantum dots surfaces. Just before the onset of Ostwald ripening, the width of the size distribution is minimized, and nanoparticles are nearly at equilibrium with the bulk monomer concentration. Under these conditions, add-atoms may be able to migrate laterally to optimize the surface structure.[1] The redistribution of material from a small particle in equilibrium with its surroundings is treated by the Gibbs-Thompson theory.

Thermodynamics or Kinetics

The combined influence of energy barriers, driving forces, material availability, and thermal mobility all affect the formation of CdSe quantum dots. The thermodynamics of a process explains which final state is preferred at equilibrium because it is more stable. If the net change in the Gibbs free energy, ΔG, is negative, this provides a strong driving force towards equilibrium.

Kinetics, on the other hand, describes the nonequilibrium rate at which a process evolves towards equilibrium. Rates often exhibit Arrhenius temperature dependence, as in Equation (3-1). In this case, the growth rate, v, of a CdSe quantum dot may be governed by the finite probability that random thermal energy at an absolute temperature, T, will enable Cd and Se components to overcome some kind of barrier, characterized by an activation energy, Q, in order to increase the size of the nanocrystal. The rate

coefficient, *r*, might also be a function of time, reactant concentrations, particle size, etc., and R_g is the Rydberg gas constant.

$$v = r_{(t,C,\ldots)} \exp\left(-\frac{Q}{R_g T}\right) \tag{3-1}$$

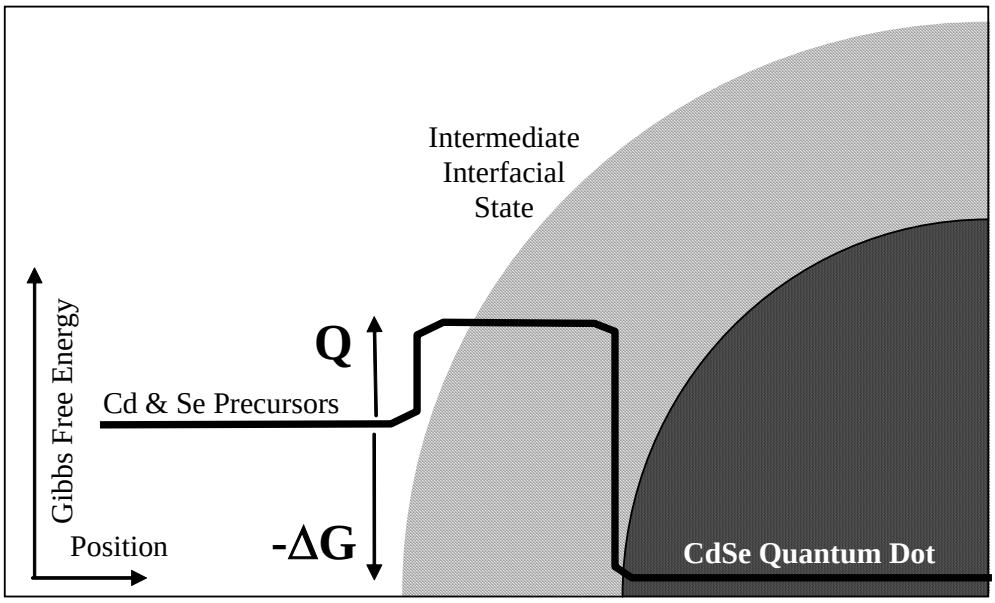

Figure 3-1. Relationship of -Δ*G* and *Q* to CdSe quantum dot formation.

The chemical reaction used to produce CdSe quantum dots by our version of the traditional TOPO method is presented in (3-2), where η is the surface area to volume ratio of the quantum dots. For the purpose of discussion, synthesis can be approximated by (3-3).

$$0.254\text{Cd-(TDPA)}_2 + 0.746\text{Cd-(TOPO)}_2 + 1.3\text{Se}^{-2} + 13.4\text{TOP} + 24.4\text{TOPO} \rightarrow \tag{3-2}$$
$$(1-\eta)\text{CdSe}_{bulk} + \eta\text{CdSe}_{surface}\text{-TDPA} + (24.4+2*0.746)\text{TOPO} +$$
$$0.5\text{TDPA} + 0.3\text{Se}^{-2} + 13.4\text{TOP}$$

$$\text{Cd(ligand)}_2 + \text{Se}^{-2} \rightarrow \text{CdSe} + 2\text{ligand} \tag{3-3}$$

In practice, the concentration of the Cd reactants becomes negligible, and the reaction goes to completion, yielding CdSe. Therefore this reaction has a large equilibrium constant, *K*, described by Equation (3-4).[60]

$$K = \exp\left(-\frac{\Delta G}{R_g T}\right) \sim \frac{[CdSe][ligand]^2}{[Cd(ligand)_2][Se^{-2}]} \tag{3-4}$$

Colloidal quantum dot formation can be divided into three stages: nucleation, growth, and ripening. During nucleation, the concentration of liquid monomer (reactants or precursors) is partially depleted by the formation many nuclei of approximately the same size. Next, particles grow by consuming the monomer. Finally, as the monomer is exhausted, the average size increases by competitive growth or ripening, when larger particles grow while smaller particles shrink and disappear, in order to reduce the net surface energy of the system.[61] During organometallic synthesis, rapid nucleation is far from equilibrium. However, the final ripening stage is closer to equilibrium, because the time scales are long and the reactant concentrations are low.

Thermodynamics of Surface Energy: Gibbs-Thompson Relation

The Gibbs-Thompson relation (3-5) is often invoked to explain particle size distributions during nucleation, growth, and ripening of quantum dots. This theory was originally developed to quantify the equilibrium between liquid droplets and a surrounding vapor, but it has been adapted to describe solid spherical nanocrystals of radius *R*, in equilibrium with a surrounding reaction solution with a monomer concentration, $C_{eq(R)}$. In this relationship, k_b is Boltzman's constant and T is the absolute temperature (in K), γ is the interfacial energy per unit area, $C_{eq(\infty)}$ is the concentration of

monomer (in molecules per unit volume) that would be in equilibrium with a flat bulk solid, and Ω_{solid} is the molecular volume of the solid material.[62]

$$C_{eq(R)} = C_{eq(\infty)} \exp\left(\frac{2\Omega_{Solid}\gamma}{R\ k_b T}\right) \tag{3-5}$$

In the Gibbs-Thompson treatment, the $1/R$ increase in the chemical potential of a quantum dot compared to the chemical potential of a bulk semiconductor originates form the increase in surface energy from dangling chemical bonds on the surface. At equilibrium, the chemical potential of the particle is the same as the chemical potential of the solution. Therefore smaller particles would be at equilibrium with higher precursor concentrations.[38]

The specific surface energy does not depend on particle radius, but rather is determined by the properties of the materials at the interface. Sugimoto derived an expression (3-6) for γ, the interfacial energy per unit area without adsorption for solid particles in a liquid, where Ω_{liquid} is the average molecular volume of the liquid.[62]

$$\gamma = -k_b T\ \ln\left\{\Omega_{liquid} C_{eq(\infty)}\right\} \Big/ \left(36\pi\ \Omega_{solid}^2\right)^{1/3} \tag{3-6}$$

The Gibbs-Thompson equation provides a conceptual starting point for discussions of some aspects of nucleation, growth, and ripening in quantum dots. Such discussions assume at least quasi-equilibrium, which might not be valid.

Nucleation occurs during initial high monomer concentrations. If nuclei randomly form with a size larger than some critical radius R^*, those radii will be energetically stable and can grow, while smaller radii would spontaneously redissolve to lower the Gibbs free energy.[38] This critical size can be estimated using thermodynamics. The free energy of formation, ΔG, is the sum of the volume energy and the surface

energy, as shown by Equation (3-7), where ρ is the density, μ_{solid} and μ_{liquid} are the chemical potentials of the bulk solid and liquid monomer, respectively. At equilibrium, the derivative of ΔG with respect to radius is zero, yielding Equation (3-8), which is similar to the Gibbs-Thompson equation.[62]

$$\Delta G = \frac{4}{3}\pi R^3 \rho\left(\mu_{solid} - \mu_{liquid}\right) + 4\pi R^2 \gamma \tag{3-7}$$

$$\rho\left(\mu_{solid} - \mu_{liquid}\right) = 2\gamma / R^* \tag{3-8}$$

To explain why focusing occurs during the growth stage, followed by widening during the ripening stage, Peng presented Equation (3-9).[29] This equation summarizes derivations made by Sugimoto, who used the Gibbs-Thompson relation (3-5) to relate the bulk and equilibrium monomer concentrations to R and R^*, respectively.[62]

$$\frac{dR}{dt} \propto D\left(\frac{1}{R} + \frac{1}{L}\right)\left(\frac{1}{R^*} - \frac{1}{R}\right) \tag{3-9}$$

During the growth stage, the monomer concentration is initially high, so that R^* is initially small, and most of the quantum dots are easily larger than $2R^*$. In this case, larger particles grow slower than smaller ones, so the smaller nanocrystals can "catch up" to the larger ones, which narrows the size distribution during growth. Equation (3-9) assumes diffusion control, which will be discussed later. Talapin extended this treatment to surface-reaction-controlled processes. He showed that for nanocrystals larger than R^* the positive rate of growth, dR/dt, is not very sensitive to nanocrystal size with reaction control.[46] Therefore reaction-limited growth is not expected to narrow the size distribution.

Later during the ripening stage of synthesis, the monomer has been consumed. Low monomer concentrations would be in equilibrium with large particles. In fact, near

equilibrium, the average nanocrystal radius is nearly equal to R^*. Only particles larger than R^* have a positive growth rate, and particles smaller than R^* shrink, so the distribution widens.[29] This last stage is called Ostwald ripening.

Kinetics of Ostwald Ripening

Foundational work in the area of Ostwald was useful but logically inconsistent. Early authors assumed that the monomer concentration is constant over time and that the total mass of the solid particles is fixed. But this violates conservation of mass; the Gibbs-Thompson relation predicts that the equilibrium monomer concentration would decrease exponentially as the average radius grows during Ostwald ripening.[61]

In a more consistent treatment, Marqusee separately compares diffusion-limited and surface-reaction-limited radial growth rates (3-10). In these equations, D is the diffusivity, V_m is the molar volume of the solid (CdSe), and k is the reaction coefficient. During Ostwald ripening, the average nanocrystal radius increases (3-11), the concentration of monomer decreases (3-12), and the total mass of the solid phase asymptotically increases.[61] Here, R_o is the radius when Ostwald ripening begins, and $C_{eq(R=\infty)}$ is the monomer concentration that would be in equilibrium with a flat bulk piece of the solid phase.

$$\frac{dR}{dt}_{diff} = \frac{DV_m}{R}\left([M_{(t)}] - C_{eq(R)}\right) \quad \text{or} \quad \frac{dR}{dt}_{reac} = k\left([M_{(t)}] - C_{eq(R)}\right) \tag{3-10}$$

$$\overline{R}_{diff} - R_o \propto t^{1/3} \quad \text{or} \quad \overline{R}_{reac} - R_o \propto t^{1/2} \tag{3-11}$$

$$\frac{[M_{(t)}]_{diff} - C_{eq(R=\infty)}}{C_{eq(R=\infty)}} \propto \frac{1}{t^{1/3}} \quad \text{or} \quad \frac{[M_{(t)}]_{reac} - C_{eq(R=\infty)}}{C_{eq(R=\infty)}} \propto \frac{1}{t^{1/2}} \tag{3-12}$$

For reaction-limited ripening, the average radius increases as the square root of time. However, during diffusion-limited ripening, the average radius increases as the cubed root of time.[61]

When the size distribution is expressed in terms of a normalized radius, $z = R/R^*$, (3-13) the normalized size distribution approaches a unique shape that depends on whether the rate-limiting mechanism is diffusion (3-15) or the surface reaction (3-16). A relative width, ω, of the distribution can be defined as the ratio of the FWHM to the most probable radius. Diffusion-limited ripening would eventually only widen the distribution moderately (ω ~ 31%) with a sharp cutoff for the largest particles. However, surface-reaction-limited ripening would approach a wider (ω ~ 86%) and more symmetric distribution of particles. Due to conservation of mass, the final distribution does not depend on the initial concentration of monomer, or the initial number of nuclei, or the growth temperature (T), although these factors would influence how fast the distribution approached its final state. In Equation (3-14), α is called the capillary length.[61]

$$z_{diff} = \frac{R}{R^*} = \frac{R}{\alpha}\left(t\frac{DV_m C_{eq(\infty)}}{\alpha^2}\right)^{-1/3} \qquad \text{or} \qquad z_{reac} = \frac{R}{R^*} = \frac{R}{\alpha}\left(t\frac{kC_{eq(\infty)}}{\alpha}\right)^{-1/2} \tag{3-13}$$

$$\alpha = 2\gamma\, V_m / k_b T \tag{3-14}$$

$$F_{diff} \propto \frac{z^2}{(2z_o - z)^{7/3}(z_o - z)^{11/3}} \exp\left\{-\frac{z}{z_o - z}\right\} \tag{3-15}$$

$$F_{reac} \propto \frac{z}{\left(\sqrt{2} - z\right)^5} \exp\left\{-\frac{3z}{\sqrt{2} - z}\right\} \tag{3-16}$$

By converting *R*, *t*, and [*M*] to dimensionless variables, Marqusee and Ross combine diffusion-limited and surface-reaction-limited cases[61] in a way that lays the groundwork for Talapin's comprehensive model, presented at the end of this chapter.[43]

Similar results are obtained by Yao,[41] but without making the power series expansion approximations of Marqusee and Ross.[61] A more accurate form is given by Equation (3-17) for the eventual normalized particle size distribution after diffusion-limited ripening.[41,46] The corresponding distribution for chemical-reaction-limited ripening is given by (3-18).[46] It is convenient that in this treatment at equilibrium, the mean radius $\overline{R}$ equals the critical radius R^*, and so the expressions (3-13) for the normalized radius simplify to $z = R/\overline{R}$.[46]

$$F_{diff} = \left(\frac{3^4 e}{2^{5/3}}\right) z^2 \frac{\exp\{-1/(1-2z/3)\}}{(z+3)^{7/3}(3/2-z)^{11/3}} \quad \text{if } 0 < z < 3/2, \text{ otherwise } F_{diff} = 0 \tag{3-17}$$

$$F_{reac} = 2^7 3z(2-z)^{-5} \exp\left\{-\frac{3z}{(2-z)}\right\} \quad \text{if } 0 < z < 2, \text{ otherwise } F_{reac} = 0 \tag{3-18}$$

For diffusion-limited ripening, if the volume fraction of spheres in solution is increased, then the mode radius remains about 12% larger than the mean radius, and the equilibrium distribution widens. Qualitatively this last point means that if synthesis is performed with lower molar ratios of reaction solvent and higher Cd and Se concentrations, then Ostwald ripening is more pronounced.[41]

We have seen how the rate-limiting mechanism affects the growth rate and the size distribution during Ostwald ripening. This information could theoretically be used to help resolve a persistent question: is the organometallic synthesis of CdSe quantum dots diffusion-controlled or reaction controlled? Since higher PLQYs and focused size distributions for narrow photoluminescence emission all occur during the *growth* stage

rather than during the *ripening* stage, it is critical to compare the potential focusing mechanisms during diffusion-limited and reaction-limited growth.

Kinetics of Reaction-Controlled Growth

If synthesis is reaction-limited, then the rate of reaction, v_{reac}, can be a function of the reactant concentrations, [Cd] and [Se], and a reaction coefficient, k, as described by Equation (3-18), for the CdSe synthesis reaction (3-3), where "δ and β are not the stoichiometric numbers in the balanced chemical equation, but have to be obtained from rate experiments."[63] Of course, k may have Arrhenius temperature dependence, characterized by an activation energy, Q, where R_g is the Rydberg gas constant, and T is the absolute temperature. The pre-exponential reaction coefficient, k_o, will have units that depend on the coefficients δ and β, and might depend on the reaction interface area. Reactant concentrations may also vary with time.

$$v_{reac} = k[Cd(ligand)_2]^{\delta}[Se^{-2}]^{\beta} = k_o \exp\left(-\frac{Q}{R_g T}\right)[Cd(ligand)_2]^{\delta}[Se^{-2}]^{\beta} \qquad (3\text{-}18)$$

The order of a reaction describes how it proceeds. In some cases, the reaction can be manipulated so that its rate depends only on the concentration of one reactant, raised to some power, p. In that case, p is the order of the reaction. If the reaction rate does not depend on concentration, but rather on the reaction surface area, the concentration in such a zero-order reaction decreases linearly with time if the reaction area is constant. In a first-order reaction, the natural log of the concentration will decrease linearly with time. In a second-order reaction, the reciprocal concentration will

increase linearly with time.[60,63] For quantum dot synthesis, these equations may need further refinement, because the total reaction surface area is not constant during growth.

If bonds are broken during a reaction, the bond strength may affect the activation energy of the reaction. Qualitatively, as discussed earlier in this chapter, the strength of the Cd-ligand bond has been shown to have a significant affect on the nucleation and growth rate. Theoretically, the metal-ligand chelate bond strength, or dissociation energy, $E_D{}^o$, at room temperature can be estimated using Equation (3-19), where $\Delta_f H^o{}_{(ligand)}$, $\Delta_f H^o{}_{(metal)}$, and $\Delta_f H^o{}_{(chelate)}$ are the enthalpy of formation of the ligand, metal, and chelate, respectively, at standard temperature and pressure.[64] Then, using Equation (3-20), the bond dissociation energy, $E_{D(T)}$, can be extrapolated to some elevated reaction temperature, T.[64]

$$E_D{}^o = \Delta_f H^o{}_{(ligand)} + \Delta_f H^o{}_{(metal)} - \Delta_f H^o{}_{(chelate)} \tag{3-19}$$

$$E_{D(T)} = E_D{}^o + 1.5R_g(T - 298) \tag{3-20}$$

Ironically, diffusion data can be used to estimate the enthalpy of formation for Cd-ligand complexes.[65] It would be insightful to compare the value of $E_{D(T)}$ to the effective activation energy, Q, for the growth phase of organometallic synthesis. However, complete thermodynamic data is often hard to find for the metal-ligand chelates used during organometallic synthesis of CdSe quantum dots.

Bullen provided a detailed quantitative analysis of the organometallic synthesis of CdSe quantum dots, based on the assumption that this is a first-order reaction-controlled process.[59] For a first-order, reaction-limited process, the growth rate is given by (3-21). Therefore during the growth phase, the growth rate is initially rapid because the total

surface area of all QDs is increasing. Later, the gradual decrease in growth rate is caused by a decrease in the concentration of monomers that are consumed during the reaction.[59]

$$\frac{d[Cd_{(t)}]}{dt} = -kA_{(t)}N_{(t)}[Cd_{(t)}] \tag{3-21}$$

Bullen used the following logic to argue that CdSe quantum dot growth is reaction-limited. He assumed standard first-order surface-reaction control and developed a model for the time it would take to form a quantum dot with given radius. By fitting the model to the radius versus time data, he extracted a reaction coefficient (in units of cm s^{-1}). Since this measured rate is 100 million times smaller than his estimate of the diffusion rate, he concludes this process is limited by the reaction rate.[59]

Despite these questions of interpretation, this model shows the expected form of the growth in the radius (3-22) for a first order reaction-limited process.[59] This is in agreement with the clear foundational work of Sugimoto. Sugimoto predicted that the standard deviation in the radius remains constant with time if the monomer concentration remains constant.[37] However, Bullen realistically took into consideration the depletion of the monomer concentration due to incorporation into a fixed number of nanocrystals with an average radius, $\overline{R}_{(t)}$.

Buried in these equations is an important contradiction. At any particular time, all of the quantum dots are in the same solution with the same concentration and the same average radius for the distribution at that time. In Equation (3-22), there is no inherent dependence on the individual radii. The $\overline{R}_{(t)}^3$ term simply corrects the bulk Cd concentration, C_{bulk}. All QDs in the distribution will experience the same rate of increase in their radius. Small and large nanocrystals will increase their radius at the same rate, so

there is no focusing mechanism for first-order surface-reaction-limited quantum dot growth, according to Bullen's equations. However, Bullen carefully tracked the steady decrease in the FWHM of PL emission, which clearly indicates there is focusing of the size distribution during growth.

$$\frac{dR_{(t)}}{dt} = kV_m\left(C_{bulk} - C_{equil}\right) = kV_m\left(C_{bulk(0)} - \frac{N_o 4\pi \overline{R}_{(t)}^{\,3}}{3V_m} - C_{equil(R)}\right) = k\left(S - \overline{R}_{(t)}^{\,3} B\right) \qquad (3\text{-}22)$$

Although first-order reaction control does not seem to provide a theoretical basis for self-narrowing size distributions, diffusion control does provide such a focusing mechanism.

Kinetics of Diffusion-Controlled Growth

Essentially, Fick's law of diffusion mathematically describes how the concentration at each point will adjust over time in order to move material down concentration gradients and to smoothly redistribute material. In spherical coordinates, this yields Equation (3-23), where x is the radial distance from the center of a sink for species with concentration C. In our case, the diffusion coefficient, D, refers to diffusion of Cd or Se precursors in the hot liquid reaction solvent surrounding a growing quantum dot.[66]

$$\frac{1}{D}\frac{\partial C}{\partial t} = \frac{2}{x}\frac{\partial C}{\partial x} + \frac{\partial^2 C}{\partial x^2} \qquad (3\text{-}23)$$

Reiss develops boundary conditions and solutions for Fick's law to treat the case of isolated liquid droplets condensing from a vapor, but claims that the results would also be useful to describe the diffusion-limited growth rate, v_{diff}, of dilute colloidal spherical particles with radius R (3-24). The concentration of precursors in the bulk liquid (more

than 10*R* away from each particle), would decrease with time as material is consumed by the growth of quantum dots according to (3-25). In this case, the rate at which R^2 increases is the same for all particles at a given time (3-26).

$$v_{diff} = 4\pi RD\left(C_{bulk(t)} - C_{\text{inter}}\right) \tag{3-24}$$

$$C_{bulk(t)} = C_o - \frac{N}{V_{org}}\frac{4\pi\overline{R}_{(t)}^3}{3V_m} \tag{3-25}$$

$$\frac{\partial R^2}{\partial t} = \frac{2V_m D}{N_A}\left(C_{bulk(t)} - C_{\text{inter}}\right) \tag{3-26}$$

From this, Reiss mathematically showed that the standard deviation of the particle size distribution narrows as particles grow under diffusion control.[66] If the concentrations remain constant (which they do not), Equation (3-26) predicts that R^2 would increase linearly with time, or that *R* would increase with the square root of time, which is a common property of simpler diffusion-limited processes.

Under some conditions, parallels between a reaction-limited growth rate, v_{reac}, (3-27) and a diffusion-limited growth rate, v_{diff}, (3-28) of solid spheres in a liquid solution with a bulk precursor concentration, C_{bulk}, can lead to questions in the interpretation of measurements. Regardless of the limiting mechanism, the growth rate of a particle should be proportional to its surface area and to the precursor concentration. Note that *k* and *D/L* both express a growth velocity (in units of cm/s). For example, the measured "reaction" rate ($k \sim 2.2 \times 10^{-6}$ cm/s) for CdSe quantum dots with oleic acid ligands and grown in a reaction solvent of octadecene at 265–275 ^{o}C [59] can be reinterpreted as a diffusion rate, *D/L*. Then the apparent diffusion coefficient would be $D \sim 5.3 \times 10^{-13}$ cm^2/s, if the effective diffusion length was approximately the length of the 18 carbon chain ligand, $L \sim 2.4 \times 10^{-7}$ cm.

$$v_{reac} \sim A\, C_{bulk} k \tag{3-27}$$

$$v_{diff} \sim A\, C_{bulk} D / L \tag{3-28}$$

This raises the question, "Do the measurements indicate a reaction-rate or a diffusion-rate limitation?" To resolve such a dispute, one would like to know the diffusion coefficient of Cd ions and Cd-oleic acid complexes through liquid octadecene or quasi-solid oleic acid ligands on the nanocrystal surface.

The diffusion coefficient for metal ions, D_M, through solid organic ligand material is significantly higher than the diffusion coefficients for metal-ligand complexes, D_{ML}, diffusing through solids of their respective ligand materials, since the complexes are much larger molecules than the ions. For example, the values of these diffusion coefficients have been measured at room temperature for Cd and the following ligands with 4-carbon chains: $D_{ML} = 2.542 \times 10^{-6}$ cm^2s^{-1} for Cd-phosphoglyceric acid, $D_{ML} = 0.521 \times 10^{-6}$ cm^2s^{-1} for Cd-phosphoenopyruvic acid, $D_{ML} = 0.854 \times 10^{-6}$ cm^2s^{-1} for Cd-nitroacetic acid, $D_{ML} = 0.751 \times 10^{-6}$ cm^2s^{-1} for Cd-acetoxyacetic acid, and $D_M = 8.345 \times 10^{-6}$ cm^2s^{-1} for Cd^{+2} through any of these ligand materials.[65] Self-diffusion coefficients for solid Cd-oleic acid have not been uncovered by the author at this time.

For Na-stearate, the self-diffusion coefficient, D_{ML}, through the liquid phase from 224 ^oC to 294 ^oC follows an Arrhenius temperature dependence, $D_{ML} = D_o \exp\{-Q/k_bT\}$, with $D_o = 2$ cm^2 s^{-1} and $Q = 0.607$ eV. Typical D_{ML} values for liquid Na-stearate are on the order of 10^{-6} cm^2 s^{-1}.[67] In the discussion section, this behavior will be compared to the kinetics of CdSe quantum dot growth in stearic acid, using Cd-stearate as a precursor.

Relationships Between Diffusion and Reaction Rates

In order to evaluate the capability of different growth modes to focus the size distribution, it is important to understand how diffusion and reaction interact via the concentration profile to control the net nucleation and growth rate (Figure 3-2).

In general, nucleation would only be expected to occur as long as the precursor concentration is above some threshold level. Since rapid nucleation consumes some precursors, the concentration would eventually go below the threshold and nucleation should stop.[37] Further growth from precursors by diffusion or reaction processes continues to reduce the concentration towards a solubility limit. Beyond this point, competitive growth modes will by definition widen the particle size distribution.[37]

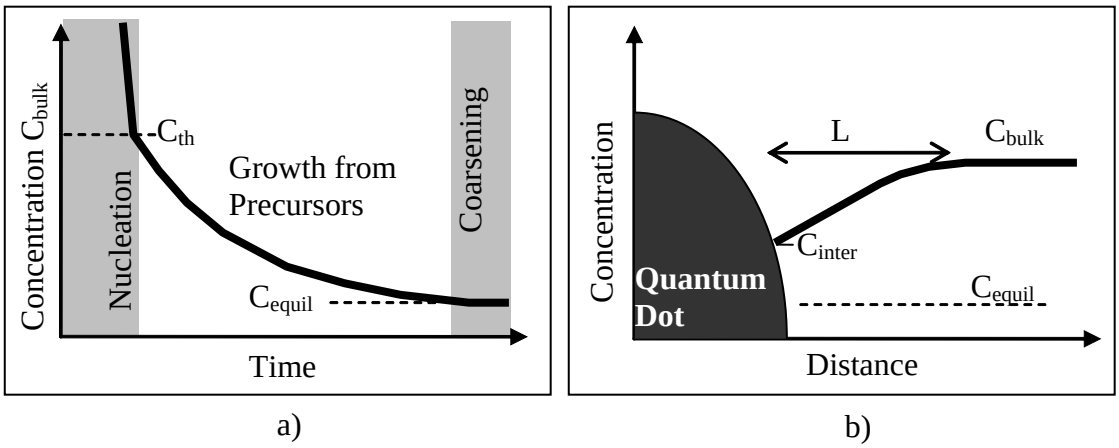

Figure 3-2. Changes in concentration for quantum dots, a) over time and b) space.

In general, both diffusion and reaction must occur in order for a quantum dot to grow. Precursors transport down the concentration gradients over a diffusion boundary layer of length *L* (3-29). Material is then incorporated into the particle at a reaction rate governed by the difference between the interface concentration and the theoretical equilibrium concentration of precursors (3-30). For conservation of mass, diffusion

growth rate, v_{diff} (in moles per second), must equal the reaction growth rate, v_{reac}, yielding the general Equation (3-31). Conservation of matter entering a spherical particle converts molar growth rate to radial growth rate (3-32).

$$v_{diff} = \left(C_{bulk} - C_{\text{inter}}\right) 4\pi DR(R+L)/L \tag{3-29}$$

$$v_{reac} = \left(C_{\text{inter}} - C_{equil}\right) 4\pi R^2 k \tag{3-30}$$

$$\frac{\left(C_{\text{inter}} - C_{equil}\right)}{\left(C_{bulk} - C_{\text{inter}}\right)} = \frac{D}{kR}\left(\frac{R+L}{L}\right) \tag{3-31}$$

$$v = \frac{4\pi R^2}{V_m}\frac{dR}{dt} \tag{3-32}$$

During diffusion-limited growth, the radius grows according to Equation (3-33). For first-order reaction-limited polynuclear layer growth, where incorporation is slower than lateral diffusion, the radial growth rate is given by (3-34).

$$\left.\frac{dR}{dt}\right|_{diff} = \left(C_{bulk(t)} - C_{equil(R)}\right) DV_m\left(\frac{1}{R_{(t)}} + \frac{1}{L}\right) \tag{3-33}$$

$$\left.\frac{dR}{dt}\right|_{reac} = \left(C_{bulk(t)} - C_{equil(R)}\right) kV_m \tag{3-34}$$

In diffusion-limited growth, since larger particles grow slower, the sizes of smaller particles can catch up with those of larger ones, which focuses the size distribution. In contrast, the reaction-limited growth rate is independent of radius, so only the relative width, $\sigma_R / \overline{R}$, of the distribution becomes smaller, not the actual standard deviation, σ_R. Therefore diffusion control can narrow the size distribution more effectively than reaction control.[37] This treatment can be improved by considering the consumption of precursors during growth.

Comprehensive Model

No discussion of quantum dot growth mechanisms would be complete without reference to Talapin's comprehensive treatment under Weller's direction,[43] which is summarized here for the reader's convenience. The net reaction rate, v_{reac} , for growth of a colloidal nanocrystal results from an imbalance between the influx of the reactants and the dissolution of the nanocrystal (3-35). B_g and B_d are the pre-exponential reaction coefficients for growth and dissolution, respectively, of a flat surface. Growth and dissolution are assumed to have a first-order and zero-order dependence on the interfacial monomer concentration, respectively. In that case, B_g and B_d will have different units. $\Delta^* \mu_g^\infty$ and $\Delta^* \mu_d^\infty$ are the activation energies for growth and dissolution, respectively, for a flat surface. ϕ is a transfer coefficient, between 0 and 1, which expresses what fraction of the surface energy actually increases the chemical potential of the nanocrystal. At the nanocrystal-solvent interface, γ is the surface energy per unit area. V_m is the molar volume of solid CdSe.[43]

$$v_{reac} = 4\pi R_{(t)}^2 \left(C_{\mathrm{inter}(t)} B_g \exp\left\{ -\frac{\Delta^* \mu_g^\infty}{R_g T} \right\} \exp\left\{ -\phi \frac{2\gamma V_m}{R_{(t)} R_g T} \right\} - B_d \exp\left\{ -\frac{\Delta^* \mu_d^\infty}{R_g T} \right\} \exp\left\{ (1-\phi) \frac{2\gamma V_m}{R_{(t)} R_g T} \right\} \right) \quad (3\text{-}35)$$

Talapin assumes that the effective diffusion distance, L, is much larger than R,[46] so that (3-29) reduces to (3-36).

$$v_{diff(t)} = \left(C_{bulk(t)} - C_{\mathrm{inter}(t)} \right) 4\pi D R \quad (3\text{-}36)$$

Following Sugimoto's treatment of mass conservation,[37] the reaction rate is equated with the diffusion rate in order to estimate how the monomer concentration at the surface of the nanocrystal, $C_{inter(t)}$, adjusts in Equation (3-37) to keep the diffusion and

reaction rates in balance as the bulk monomer concentration, $C_{bulk(t)}$, decreases with time.[43]

$$C_{\text{inter(t)}} = \frac{DC_{bulk(t)} + R_{(t)}B_d \exp\left\{-\frac{\Delta^* \mu_d^\infty}{R_g T}\right\}\exp\left\{(1-\phi)\frac{2\gamma V_m}{R_{(t)}R_g T}\right\}}{D + R_{(t)}B_g \exp\left\{-\frac{\Delta^* \mu_g^\infty}{R_g T}\right\}\exp\left\{-\phi\frac{2\gamma V_m}{R_{(t)}R_g T}\right\}} \tag{3-37}$$

Within this framework, modeling the evolution of nanocrystal size involves solving a differential equation (3-38), which uses the following four dimensionless quantities: $R^* = R_{(t)}R_g T/(2\gamma V_m)$, $\tau = tR_g^2 T^2 D\, C_{flat}^o/(4\gamma^2 V_m)$, $K = R_g TD/(2\gamma V_m k_g^{flat})$, and $S = C_{bulk}/C_{flat}^o$, where C_{flat}^o and k_g^{flat} are described by Equations (3-39) and (3-40), respectively. One of the strengths of this approach is that growth during mixed control can be evaluated as the parameter *K* changes from 0.001 for diffusion control to 1000 for reaction control.[43]

$$\frac{dR^*}{d\tau} = \frac{S - \exp\{1/R^*\}}{R^* + K\exp\{\alpha/R^*\}} \tag{3-38}$$

$$C_{flat}^o = \frac{B_d}{B_g}\exp\left\{\frac{\Delta^* \mu_g^\infty - \Delta^* \mu_d^\infty}{R_g T}\right\} \tag{3-39}$$

$$k_g^{flat} = B_g \exp\left\{-\frac{\Delta^* \mu_g^\infty}{R_g T}\right\} \tag{3-40}$$

Since this differential equation (3-38) does not have an analytical solution, Talapin did extensive Monte Carlo simulations to predict radial growth rates as a function of nanoparticle size. Talapin's simulations of the equilibrium nanocrystal size distributions after Ostwald ripening agree with Yao's expressions in reaction (3-17) and diffusion (3-18) limiting cases.[41,46]

During the growth stage of typical organometallic synthesis, Talapin's equation (3-35) can be simplified to (3-41) by assuming that the rate of growth is significantly faster than the rate of dissolution (*i.e.* $B_g >> B_d$) during growth. If we are not sure about the relative scale of L versus R, we could revert back to the more general form of the diffusion rate (3-29). Then the mass balance argument would yield Equation (3-42). Including Arrhenius behavior for diffusivity of the form $D = D_o e^{-Q_D / R_g T}$, where Q_D is the diffusion activation energy, gives a useful expression for the ratio of the bulk and the interfacial monomer concentrations (3-43) for analyzing quantum dot growth kinetics.

$$v_{reac} = 4\pi R^2 C_{\text{inter}} B_g \exp\left\{-\frac{\Delta^* \mu_g^\infty - \phi 2\gamma V_m / R}{R_g T}\right\} \tag{3-41}$$

$$C_{\text{inter}} R B_g \exp\left\{-\frac{\Delta^* \mu_g^\infty - \phi 2\gamma V_m / R}{R_g T}\right\} = \left(C_{bulk} - C_{\text{inter}}\right) D(R+L)/L \tag{3-42}$$

$$\frac{C_{bulk}}{C_{\text{inter}}} = 1 + \frac{R B_g L}{D_o (R+L)} \exp\left\{\frac{Q_D - \Delta^* \mu_g^\infty + \phi 2\gamma V_m / R}{R_g T}\right\} \tag{3-43}$$

Building on a wealth of recent on CdSe quantum dot research, there are opportunities for new contributions. Experimentally, benchmark organometallic synthesis methods have been established, and a wide range of alternative solvents are being explored. But, synthesis activation energies need to be measured for these solvents. At this point, the mathematical treatments of Ostwald ripening are more mature than those of growth. To commercialize quantum dot synthesis, there is a need for self-consistent analytical expressions describing the evolution of photoluminescence and absorbance peak wavelength as a function of synthesis time, temperature, and reactant concentration.